Antibody-Dependent Enhancement of IL-6 Production by SARS-CoV-2 Nucleocapsid Protein

Emi E. Nakayama (emien@biken.osaka-u.ac.jp)
Osaka University
Ritsuko Kubota-Koketsu
Osaka University
Tadahiro Sasaki
Osaka University
Keita Suzuki
TANAKA Kikinzoku Kogyo K.K
Kazuko Uno
Louis Pasteur Center for Medical Research
Jun Shimizu
MiCAN Technologies Inc
Toru Okamoto
Osaka University
Hisatake Matsumoto
Osaka University
Hiroshi Matsuura
Osaka Prefectural Nakakawachi Emergency and Critical Care Center
Shoji Hashimoto
Osaka Prefectural Hospital Organization Osaka Habikino Medical Center
Toshio Tanaka
Osaka Prefectural Hospital Organization Osaka Habikino Medical Center
Hiromasa Harada
Yao Tokushukai General Hospital
Masafumi Tomita
Kobe Tokushukai Hospital
Mitsunori Kaneko
Suita Tokushukai Hospital
Kazuyuki Yoshizaki
Osaka University
Tatsuo Shioda
Osaka University

Research Article

Keywords: SARS-CoV-2, N protein, cytokine storm, monoclonal antibody, IL-6, COVID-19, macrophage

Posted Date: February 17th, 2022

DOI: https://doi.org/10.21203/rs.3.rs-1320609/v1

Abstract

A cytokine storm induces acute respiratory distress syndrome, the main cause of death in coronavirus disease 2019 (COVID-19) patients. However, the detailed mechanisms of cytokine induction due to severe acute respiratory syndrome coronavirus 2 (SARS-CoV-2) remain unclear. To examine the cytokine production in COVID-19, we mimicked the disease in SARS-CoV-2-infected alveoli by adding the lysate of SARS-CoV-2-infected cells to cultured macrophages or induced pluripotent stem cell-derived myeloid cells. The cells secreted interleukin (IL)-6 after the addition of SARS-CoV-2-infected cell lysate. Screening of 25 SARS-CoV-2 protein-expressing plasmids revealed that the N protein-coding plasmid alone induced IL-6 production. The addition of anti-N antibody further enhanced IL-6 production, but the $F(ab')^2$ fragment did not. Sera from COVID-19 patients also enhanced IL-6 production, and sera from patients with severer disease induced higher levels of IL-6. These results suggest that anti-N antibody promotes IL-6 production in SARS-CoV-2-infected alveoli, leading to the cytokine storm of COVID-19. (150 words)

Introduction

Severe acute respiratory syndrome coronavirus 2 (SARS-CoV-2) is a causative agent of coronavirus disease 2019 (COVID-19) [1]. The surface of the virus particle is covered with spike (S) proteins, and the envelope contains membrane and envelope proteins. The internal genetic information is coded in a positive-sense single-stranded RNA approximately 30 kb in length, which is the largest known viral RNA, and the RNA forms a complex with nucleocapsid (N) proteins.

The receptor of SARS-CoV-2 is angiotensin-converting enzyme 2 (ACE2) [2], which also serves as a receptor for the common cold coronavirus NL63 and severe acute respiratory syndrome coronavirus (SARS-CoV), a coronavirus that is closely related to SARS-CoV-2 [1]. The ACE2 is highly expressed in the intestinal tract, testicles, kidney, heart, salivary gland, lung, liver, oral cavity, and nasal mucosa. Although there is a possibility of the infection of macrophages [3] and vascular endothelial cells [4], the virus levels in blood are not high [5], so the vasculitis and cytokine storm associated with COVID-19 may have immunological mechanisms beyond direct viral involvement.

Numerous cytokines and chemokines have been associated with the acute respiratory distress syndrome caused by SARS[6] and SARS-CoV-2[7–9]. Among these cytokines, interleukin (IL)-6 is particularly important for predicting the disease severity[10,11]. Monocytes, which are one of the main sources of this cytokine at inflammatory sites[12], are found in large numbers in the bloodstream, and are often the first cells of the immune system to come into contact with virus particles[13].

The virus can theoretically replicate in human macrophages and dendritic cells, triggering the aberrant production of proinflammatory cytokines/chemokines, if all components of viral binding and activation are available[14]. Regarding Middle East respiratory syndrome (MERS) coronavirus, another coronavirus that is less closely related to SARS-CoV-2 than SARS-CoV, it was reported that the viral RNA levels increased in the culture supernatant for 3 days, but that the infectivity of the supernatant dropped during

these 3 days[15]. Yilla et al. examined the replication of SARS-CoV in purified monocytes/macrophages, and found that SARS-CoV replicated poorly[16], although preliminary electron microscopic studies demonstrated that SARS-CoV-like particles could enter the cells, possibly via phagocytosis. Despite the abortive infection of SARS-CoV[17,18], which is characterized by infection without replication, SARS-CoV infection of human macrophages induced the expression of proinflammatory chemokines, such as IP-10 and MCP-1, whereas antiviral cytokine IFN-β production was largely absent[3,19]. Interestingly, tissue resident macrophages infected with SARS-CoV-2 were found in the bronchoalveolar lavage fluid of acute respiratory distress syndrome patients[20]. Significant expansion of the population of CD14+CD16+ monocytes producing IL-6 was also observed in the peripheral blood of patients with COVID-19 in intensive care units when compared to COVID-19 patients who did not require hospitalization in an intensive care unit[21]. These observations prompted us to investigate the mechanisms of the expression of IL-6 in peripheral monocyte-derived macrophages (MDM) infected with SARS-CoV-2. Here, we demonstrate the N protein-mediated induction of IL-6, which was further enhanced by specific antibodies against N protein.

Results

SARS-CoV-2-infected cell lysates induce IL-6 production from MDM

We first examined whether or not peripheral blood MDM could be productively infected with SARS-CoV-2. Results showed virtually no SARS-CoV-2 growth in MDM differentiated with GM-CSF (Figure 1A) or M-CSF (Figure 1B and S1A). Production of IL-6 was also not observed after simple inoculation of SARS-CoV-2 (Figure S2). These results were similar to those of a recent report [22]. We then examined the effects of SARS-CoV-2-infected cells on MDM as a model of SARS-CoV-2 infection in alveoli. Since MDM would contact components of epithelial cells in SARS-CoV-2-infected alveoli, we added freeze/thawed lysates of TMPRSS2/VeroE6 cells infected with SARS-CoV-2 to MDM together with SARS-CoV-2. Although the levels of SARS-CoV-2 RNA decreased over time (Figure S2), elevated levels of IL-6 were detected in the supernatants of MDM incubated with SARS-CoV-2-infected cell lysate, but not in those with uninfected cell lysate (Figure 1C and S2). Three different strains of SARS-CoV-2 isolates were able to induce IL-6 (Figure S2).

For further analysis, we tested K-ML2 cells as a substitute for MDM. K-ML2 cells are induced pluripotent stem (iPS) cell-derived myeloid cells expressing genetically engineered GM-CSF and M-CSF[23]. As expected, the SARS-CoV-2-infected cell lysates could induce IL-6 production from K-ML2 cells, and further addition of SARS-CoV-2 was not required for IL-6 induction in both MDM and K-ML2 cells (Figure 1C). These results suggested that a certain component in SARS-CoV-2-infected cells stimulated MDM and K-ML2 cells to produce IL-6.

SARS-CoV-2 N protein induces IL-6 production more efficiently than S protein

We speculated that the SARS-CoV-2 S protein induced IL-6. Addition of recombinant S protein at a final concentration of 1000 ng/mL did indeed induce IL-6 at a level comparable to that induced by the SARS-CoV-2-infected cell lysate (Figure S1B). However, the level of S protein in the SARS-CoV-2-infected cell lysate used in our experiment was only 10 ng/mL, suggesting that factor(s) other than S protein was responsible for the IL-6 induction. Screening of 25 SARS-CoV-2 protein-expressing plasmids transfected into 293T cells revealed that the N protein-coding plasmid alone induced IL-6 production (Figure 2A and 2B). Recombinant N protein also induced IL-6, and could induce much higher levels of IL-6 than the recombinant S protein (Figure 2C).

To identify the specific domain in the N protein that is responsible for inducing IL-6 production, we constructed plasmids encoding truncated versions of the N protein (Figure 2D and 2E). The specific domain responsible for inducing IL-6 was located in the C-terminal domain (CTD) of the N protein, since IL-6-inducing activity was found in the cell lysate containing the CTD of the N protein (Figure 2F). The N-terminal domain (NTD) of the N protein did not stimulate an increase in IL-6 from the basal level (Figure 2F).

N protein induces the production of multiple cytokines, including IL-8, from peripheral MDM

The levels of IL-6, IL-8, and TNF-α are known to be elevated in severe COVID-19 cases [24–26]. The culture supernatants of MDM 2 days after N protein stimulation were assayed for the levels of the cytokines and chemokines shown in Table S1. We found that the levels of multiple cytokines, including IL-6, IL-8, TNF-α, MIP-1β, RANTES, GRO α, pentraxin-3, and TSLP, were elevated after the addition of N protein in both GM-CSF-stimulated and M-CSF-stimulated MDM (Table S1 and Figure 3A). In the case of IP-10, which was previously proposed as a predictive marker for severe disease in COVID-19 [27], an N protein-induced increase was observed only in GM-CSF-stimulated MDM, but not in M-CSF-stimulated MDM (Figure 3B). These findings indicated that MDM can be a source of cytokines in COVID-19 patients even without productive infection of SARS-CoV-2.

Anti-N protein monoclonal antibodies enhance IL-6 production via the Fc-receptor

We added S2-2-5 monoclonal antibody (mAb) against N protein (S2) to neutralize the N protein that induced IL-6 production. Contrary to our expectation, the anti-N protein mAb enhanced the IL-6 production (Figure 4A). This enhancing activity was found to be Fc-receptor-dependent, since the F(ab')2 form of the S2 mAb did not enhance IL-6 production (Figure 4B). We then obtained 15 mAbs against N protein, as listed in the Key Resources Table, and tested their reactivity to the entire N protein, NTD, and CTD by enzyme-linked immunosorbent assay (ELISA). Four mAbs (C1 to C4) reacted with the N protein and CTD,

and seven mAbs (N2, N5, N6, N7, N8, N10, and N11) reacted with the N protein and NTD. Two mAbs (N1 and N4) reacted only with the N protein, and two mAbs (N9 and N12) reacted with the N protein and NTD, and weakly with the CTD (Figure 4C). All four mAbs that bound to the CTD enhanced the IL-6 production, while six of the nine mAbs that bound to the NTD enhanced the IL-6 production (Figure 4D). Interestingly, two mAbs (N1 and N4) lacking reactivity with both the CTD and NTD only weakly enhanced the IL-6 production (Figure 4D). Similar to the S2 mAb, the F(ab')2 form of the S2 mAb retained reactivity to the N protein (Figure 4C). These results suggested that the anti-N antibody enhanced the uptake of N protein into macrophages via the Fc-receptor.

Patient sera from severe COVID-19 cases enhance the IL-6 production induced by N protein

To determine whether or not anti-N antibodies that are raised from actual SARS-CoV-2 infection can also enhance the IL-6 production induced by N protein, we added serially diluted patient sera to K-ML2 cells with N protein. We found that 0.01–10% of the COVID-19 patient sera clearly enhanced the IL-6 production induced by N protein (Figure 4E). The addition of sera from five healthy donors did not affect the IL-6 production (Figure S2). We then evaluated a total of 203 serum samples from 63 mild, 43 moderate I, 40 moderate II, and 55 severe COVID-19 cases. We found that sera from the severe cases induced significantly more IL-6 than those from the other cases (Figure 4F). The levels of anti-N antibodies in the sera also tended to be elevated in the severe cases (Figure S1C).

Discussion

It is well-known that the course of COVID-19 varies among individuals, and that the medical condition of patients suddenly worsens at 5 to 8 days after the onset of symptoms [5,28,29]. This disease course suggests the involvement of certain acquired immune responses to SARS-CoV-2, but the precise mechanisms of the rapid disease progression are not well understood. Several previous studies have shown that the anti-N antibody levels were positively correlated with the disease severity [30,31]. In the present study, we showed that the N protein produced in infected epithelial cells which were refractory to virus production, can induce IL-6 production from bystander macrophages or myeloid cells, and that antibodies against N protein enhanced this phenomenon.

Recently, Kawaciak et al. reported that both the S and N proteins of SARS-CoV-2 induced IL-6 in monocytes and macrophages by using 1000 ng/mL of recombinant proteins [32]. Zhang et al. previously showed that an 80-amino acid residue of the C terminus of the SARS N protein was required for IL-6 production via the transcription factor nuclear factor-kB [33]. During the preparation of our manuscript, Pan et al. reported that the CTD of the SARS-CoV-2 N protein interacts with NOD-, LRR- and pyrin domain-containing protein 3 (NLRP3) to activate inflammasomes and the NF-kB pathway [34]. Our results also showed the importance of the C terminal portion of the N protein for inducing IL-6. In addition, we clarified that the N protein has a higher potency to induce IL-6 than the S protein, and proposed that Fc-receptor-dependent and anti-N-antibody-dependent enhancement of IL-6 may be a trigger of cytokine storm.

Antibody-dependent enhancement (ADE) of coronavirus infection was first reported in feline infectious peritonitis virus [35], and it has been thought to enhance the infection of SARS-CoV in macrophages via the Fc-receptor [36]. Phenomena similar to ADE have been observed in multiple SARS-CoV animal models. In a mouse model, attempts to create vaccines against SARS-CoV led to pulmonary immunopathology upon challenge with SARS-CoV [37,38]; these vaccines included inactivated whole viruses, inactivated viruses with adjuvant, a recombinant S protein, and a mouse hepatitis coronavirus-like particle vaccine, and the vaccinated mice showed increased eosinophilic proinflammatory pulmonary responses upon challenge. Severe pneumonia was observed in mice vaccinated with N protein after challenge with SARS-CoV [39]. Based on these findings and our results, we propose that ADE of cytokine production from macrophages occurs even without productive infection.

Our proposed mechanism for the ADE of IL-6 production can explain why most of the previously developed vaccines against SARS-CoV and MERS viruses failed to elicit protective immunity against these viruses. Furthermore, our finding is consistent with the fact that the efficacy of inactivated vaccines against severe COVID-19 is lower than that of mRNA-based vaccines [40,41]. In addition, our model is also consistent with the fact that therapy with convalescent plasma, which contains anti-N antibodies, failed to improve the disease course in several studies[42–44].

There is controversy whether vaccination is necessary in SARS-CoV-2-infected individuals and in those who have already recovered from SARS-CoV-2 infection [45]. Our results suggest that vaccination with an mRNA-based or adenovirus-based vaccine, which induces an anti-S protein immune response alone, would be highly recommended for those who have previously been infected with SARS-CoV-2, since the pre-existing anti-N protein antibody may be a risk factor for the development of a cytokine storm if they get infected with SARS-CoV-2 again. It would be safer to generate an inactivated whole virus vaccine in which N protein epitopes are engineered not to bind to enhancing anti-N antibodies.

It was observed that pre-existing memory B cells to other human coronaviruses, such as OC43 and HKU-1 [46], might respond to SARS-CoV-2 rapidly [31,47,48]. Early high antibody responses are correlated with increased disease severity in both SARS [49] and COVID-19 [24,50–53]. As described above, the anti-N antibody levels are correlated with the disease severity [30,31]. In addition, it is well-known that an age over 65 years is a risk factor for severe COVID-19 [54]. Gorse et al. reported that the levels of antibodies to coronaviruses were higher in older adults than in younger adults [47]. Li et al. analyzed the anti-SARS-CoV-2-specific IgG levels in COVID-19 patients according to age, and found that the most significant difference in the levels of anti-N antibody during hospitalization was observed between those aged <65 years and those aged >65 years[48]. Our results may explain why elderly people, who are more likely to have been previously exposed to human common cold coronaviruses, experience more severe COVID-19 than the younger generation.

Regarding the treatment of patients, steroids, anti-IL-6 receptor antibody[55], or anti-JAK treatment [56] are recommended to suppress excessive immune responses. NLRP3 signal inhibitors was also proposed as

candidate drugs[34]. However, these treatments increase the risk of other infections, including those by bacteria and fungi, since they suppress the host immune defense. In the present study, we used 16 mAbs against N protein, and found that five antibodies did not enhance IL-6 production while 11 did. These five antibodies (N1, N4, N5 N9, and N12) may be useful as starting materials for novel treatment strategies for COVID-19. Although further studies are necessary to establish treatments for COVID-19 by suppressing IL-6, macrophage stimulation by N protein should be avoided to prevent the development of cytokine storm.

Methods

Human materials

This study followed the principles of the Declaration of Helsinki, and was approved by the institutional review board of Osaka University Hospital (No. 885). Informed consent for the collection of blood samples was obtained from the patients or their relatives. The use of left-over specimen of daily test after anonymization was approved by the institutional review board of Habikino Medical Center (150-7), Louis Pasteur Center for Medical Research (LPC29), and Tokushukai Hospital (TGE01547). A brief summary of the protocol was disclosed. The use of human blood from healthy volunteers in this study was approved by the Research Ethics Committee of the Research Institute for Microbial Diseases, Osaka University, Japan (No. 2021-3).

Animals

The animal study was carried out in accordance with the recommendations in the guide for the care and use of laboratory animals of Osaka University, Japan. Our protocol was approved by the Committee on the Ethics of Animal Experiments of the Research Institute for Microbial Diseases, Osaka University, Japan (No. R01-17-0). All procedures in this animal experiment were conducted in a manner to avoid or minimize discomfort, distress or pain to the animals according to ARRIVE guidelines (https://arriveguidelines.org/), and the approved operating procedures and guidelines at the Research Institute for Microbial Diseases of Osaka University.

Viruses and cells

SARS-CoV-2 (KNG19-020) was kindly supplied by Dr. Tomohiko Takasaki of the Kanagawa Prefectural Institute of Public Health. SARS-CoV-2 (JPN-TY-WK-521) was obtained from the National Institute for Infectious Diseases, Japan. Clinical isolates hCoV-19/Japan/OIPH14/2020 and hCoV-19/Japan/OIPH21/2020 [57] were propagated in TMPRSS2/VeroE6 cells [58] that were obtained from the National Institutes of Biomedical Innovation, Health and Nutrition, Japanese Collection of Research Bioresources Cell Bank, Japan. K-ML2 cells were established as described previously [59] and maintained in minimum essential medium supplemented with 10% fetal calf serum. Peripheral blood mononuclear cells were obtained from the blood buffy coats of healthy donors by Ficoll-Paque density gradient centrifugation, then plated in 24-well MULTIWELL™ PRIMARIA™ plates (Becton Dickinson, Franklin Lakes, NJ) containing RPMI 1640 supplemented with 10% fetal calf serum. Monocytes were differentiated into

macrophages for 8 days in the presence of 100 ng/mL of GM-CSF (PeproTECH, Rocky Hill, NJ) or 50 ng/mL of M-CSF (PeproTECH). To prepare SARS-CoV-2 infected cell lysates, TMPRSS2/VeroE6 cells were infected with SARS-CoV-2 at a multiplicity of infection of 0.01, and the cells were harvested 16 h after infection. Subsequently, 1.6×10^5 infected cells were suspended in 200 μL of phosphate-buffered saline (PBS) and frozen at -20°C. After thawing, 10 μL of suspended cell lysate was added to 100 μL of culture medium in each well containing macrophage or K-ML2 cells with or without SARS-CoV-2 and diluted serum. After 4 h of incubation, macrophages were washed once with culture medium, then 500 μL of fresh medium was added, and the cells were cultivated for 2 days at 37°C under an atmosphere of 5% CO_2.

Real-time RT-PCR

Viral RNA was extracted from 140 μL of culture supernatant using the QIAamp Viral RNA Mini Kit (QIAGEN, Hilden, Germany) according to the manufacturer's instructions. Real-time quantitative reverse transcription PCR (RT-qPCR) assays were performed using the One Step TB Green® PrimeScript™ RT-PCR kit II (Takara, Shiga, Japan) and the SYBR Green assay 2 primer sets designed by MilliporeSigma (https://www.sigmaaldrich.com/US/en/technical-documents/protocol/research-and-disease-areas/immunology-research/ncov-coronavirus). The components of the RT-qPCR reaction mixture were as follows: 6.25 μL of 2× One Step SYBR® RT-PCR Buffer 4, 0.25 μL of forward primer (10 μM), 0.25 μL of reverse primer (10 μM), 0.25 μL of ROX reference Dye II (50×), 2.5 μL of deionized water, 0.5 μL of PrimeScript 1 step Enzyme Mix 2, and 2.5 μL of template RNA. Reverse transcription was performed at 42°C for 5 min, followed by denaturation at 95°C for 10 min, and 40 amplification cycles at 95°C for 5 s and 60°C for 34 s. A Quant Studio 3 Real-Time PCR System (Life Technologies, Carlsbad, CA) was used for the analysis.

IL-6 measurement

Serially diluted S protein (Spike S1+S2 ECD-His Recombinant Protein, 40589-V08B1, Sino Biological, Beijing, China), N protein (40588-V08B or 40588-V07E, Sino Biological), or 10 μL of cell lysate suspended in 100 μL of culture medium was added to 100 μL of the K-ML2 cell suspension or monocyte-derived macrophages with 100 μL of culture medium and incubated at 37°C for 4 h. Then, 500 μL of fresh medium was added to the wells. Two days later, the culture supernatants were harvested, and the levels of IL-6 were measured by an enzyme-linked immunoassay (ELISA MAX Deluxe Set Human IL-6, BioLegend, San Diego, CA).

Plasmid construction and transfection

We used standard molecular biology techniques for cloning and plasmid construction. Most of the plasmid constructs were generated in the pLVX-EF1alpha-SARS-CoV-2-N-2xStrep-IRES-Puro vector backbone (for more details, see the Key Resources Table). A standard transfection reagent, TransIT-293 transfection reagent (V2704, Takara), was used.

Western blot

Plasmid-transfected 293T cells (6×10^5 cells) were lysed in 100 µL of lysis buffer (50 mM Tris–HCl at pH 7.5, 150 mM NaCl, 1% Nonidet P-40, and 0.5% sodium deoxycholate). Proteins in the lysates were subjected to sodium dodecyl sulfate-polyacrylamide gel electrophoresis. The proteins in the gel were then electrically transferred to a membrane (Immobilion; Millipore, Billerica, MA). Blots were blocked and probed with N2 mAb (HM1057, EastCoast Bio, Maryland Hights, MO) or C2 mAb (CV15, CerTest Biotec, Zaragoza, Spain) overnight at 4°C. The blots were then incubated with peroxidase-linked anti-mouse IgG (H+L), and the bound antibodies were visualized with a Chemi-Lumi One chemiluminescent kit (Nacalai Tesque, Kyoto, Japan).

Immunization, fusion, and selection of mAb

SARS-CoV-2 (KNG19-020) was propagated in TMPRSS2/VeroE6 cells (JCBR1819) and purified by sucrose gradient centrifugation [60]. Concentrated virus was then exposed to ultraviolet light (0.6 J/cm^2) to inactivate the virus. We confirmed that the virus had completely lost its infectivity by this method. BALB/c mice (4 weeks old, female) were intraperitoneally immunized three times by the inactivated virion (corresponding to 3.8×10^7 TCID50/mouse) with adjuvant (1st immunization: Freund's complete adjuvant (WAKO, Tokyo, Japan); 2nd and 3rd immunization: Freund's incomplete adjuvant (WAKO)). Three days after the last immunization, splenic cells from the mice were used to prepare hybridomas. The hybridoma-producing mAbs were generated as described previously [61] using mouse myeloma PAI cells. The antibodies secreted by the hybridomas were screened by an indirect immunofluorescence assay using SARS-CoV-2-infected cells. SARS-CoV-2-infected and mock-infected TMPRSS2/VeroE6 cells were cultured for 18 h, fixed with 7% formaldehyde-PBS for 30 min, and then permeabilized with 1% Triton X-100 PBS for 5 min. The cells were incubated with hybridoma culture supernatant at 37°C for 1 h, followed by incubation with goat anti-mouse IgG conjugated to Alexa Flour 488 (1:1000; Invitrogen, Carlsbad, CA) for 30 min at 37°C. The cells were observed under a fluorescence microscope (ECLIPSE Ti2, Nikon, Tokyo, Japan). The isotype of the antibodies was determined by an IsoStrip™ mouse Monoclonal Antibody Isotyping kit (Roche, Mannheim, Germany). The target of the antibodies was determined by the staining patterns using an indirect immunofluorescence assay and the reactivity to N protein-expressing cells.

ELISA for S protein

The amount of S protein in the SARS-CoV-2-infected cell lysates was measured by a SARS-CoV-2 Spike Protein ELISA kit (E-EL-E605, Elabscience, Houston TX) according to the manufacturer's instructions.

In-house ELISA of anti-N antibodies

Ninety-six-well flat-bottom microplates were coated with 100 ng/well of N protein (40588-V08B, Sino Biological), NTD (40588-V07E10, Sino Biological), or CTD (40588-V07E5, Sino Biological) in 50 µL of carbonate-bicarbonate buffer (C-3041, Sigma, St. Louis, MZ), and incubated at 4°C overnight. After washing with 0.05% Tween 20 in PBS (PBS-T), wells were blocked with 200 µL of a 25% solution of BlockAce for 1 h at room temperature. After washing with PBS-T, 100-times diluted patient serum with PBS-T or mouse mAb (1 µg/mL), as listed in the Key Resources Table, was added and incubated for 1 h at room temperature. After washing with PBS-T, 50 µL of the secondary antibody solution of peroxidase-

conjugated AffiniPure alpaca anti-Human IgG (H+L) (609-035-213, Jackson ImmunoResearch, Pennsylvania, PA) or peroxidase-labeled goat anti-mouse IgG (H+L) (5220-0341, CeraCare, Milford, MA) was added and incubated for 1 h at room temperature. A TMB substrate kit (34021, Thermo Fisher Scientific, Waltham, MA) was used for colorimetric detection, and the optical density at 450 nm was measured by a Multigrading Microplate Reader (SH-9500Lab, Corona, Hitachinaka, Ibaraki, Japan).

Multiplex cytokine measurement

Cytokine and chemokine biomarkers were quantified using the Bio-Plex 200 multiplex cytokine array system (Bio-Rad Laboratories, Hercules, CA) according to the manufacturer's instructions. Serum samples were collected from patients and centrifuged at 1600 *g* for 10 min. The serum samples were frozen at −80°C until they were analyzed.

We simultaneously quantified cytokines, chemokines, and soluble receptors using the Bio-Plex Human Cytokine 27-plex Panel (IL-1β, IL-1Rα, IL-2, IL-4, IL-5, IL-6, IL-7, IL-8, IL-9, IL-10, IL-12 (p70), IL-13, IL-15, IL-17A, eotaxin, basic fibroblast growth factor, G-CSF, GM-CSF, IFN-γ, IP-10, MCP-1, MIP-1α, platelet-derived growth factor-BB, MIP-1β, RANTES, TNF-α, and vascular endothelial growth factor; (Bio-Rad Laboratories, Hercules, CA), the Inflammation Panel (a proliferation-inducing ligand (APRIL), B-cell activation factor, soluble CD30, soluble CD163, chitinase, soluble glycoprotein 130, IFN-α2, IFN-β, IFN-γ, IL-2, IL-8, soluble IL-6 receptor α, IL-10, IL-11, IL-12 (p40), IL-12 (p70), IL-19, IL-20, IL-22, IL-26, IL-27, IL-28A, IL-29, IL-32, IL-34, IL-35, lymphotoxin-like inducible protein that competes with glycoprotein D for herpesvirus entry on T cells (LIGHT), matrix metalloproteinase (MMP)-1, MMP-2, MMP-3, osteocalcin, osteopontin, pentraxin-3, soluble TNF receptor 1, soluble TNF receptor 2, thymic stromal lymphopoietin, and TNF-like weak inducer of apoptosis; Bio-Rad Laboratories), and the Bio-Plex pro (hepatocyte growth factor, IL-18, TNF-related apoptosis-inducing ligand, IL-2 receptor α, M-CSF, growth-related oncogene α, MCP-3, and monokine induced by IFN-γ; (Bio-Rad Laboratories, Hercules, CA). Data acquisition and analysis were performed using Bio-Plex Manager software version 5.0. (Bio-Rad Laboratories, Hercules, CA).

Patient sera

The disease severity of patients was determined at hospital admission according to The Guideline for Medical Treatment of COVID-19 in Japan (https://www.mhlw.go.jp/content/000785119.pdf)

Briefly, patients with "mild" illness showed one or some of the signs and symptoms of COVID-19 (e.g., fever, cough, sore throat, malaise, headache, muscle pain, nausea, vomiting, diarrhea, and loss of taste and smell), but lacked shortness of breath, dyspnea on exertion, and abnormal imaging findings. "Moderate I" cases showed evidence of lower respiratory disease with a percutaneous oxygen saturation (SpO2) of >93% on room air, and were compatible with "moderate illness" described in the Coronavirus Disease 2019 (COVID-19) Treatment Guidelines of the National Institutes of Health (NIH; https://www.covid19treatmentguidelines.nih.gov). "Moderate II" cases were supported with non-invasive mechanical ventilation or supplemental oxygen (including high-flow oxygen devices), and were compatible with "severe illness" described in the NIH guidelines. "Severe" cases were admitted into the intensive care unit or supported with invasive mechanical ventilation or extracorporeal membrane

oxygenation, and were compatible with “critical illness” described in the NIH guidelines. In Japan, invasive ventilation was not applicable for several terminal cases. Aliquots of patient sera were collected from the leftover specimens of daily tests, and kept at -80°C until use. The median age among the 63 mild, 43 moderate I, 40 moderate II, and 55 severe cases was 57 (interquartile range, 37 – 72.5), 70 (56.5 – 80.75), 75.5 (58.25 – 85), and 69 (58.25 – 79) years, respectively. The number of males was 33 (52.4%), 22 (51.2%), 23 (57.5%), and 41 (74.5%), respectively.

Quantification and statistical analysis

The numbers of repetitions of specific experiments are shown in the figure legends. For multiple comparisons, statistical analysis was performed by the Kruskal-Wallis and Mann Whitney U tests (GraphPad Prism version 9.0.2, GraphPad Software, San Diego, CA) where applicable (Figure 4F).

Declarations

Acknowledgements

We thank all patients, physicians, nurses, and laboratory technicians at the hospitals. This work was supported by funding from the Japan Agency for Medical Research and Development (JP20nf010162 and JP20nk0101602).

Author contributions

Conceptualization: Tat.S. and E.E.N;

Investigation: E.E.N., Tad.S., and K.U.;

Resources: R.K., K.S., T.O., and J.S.;

Writing-Original Draft: E.E.N.;

Writing-Review & Editing: Tat.S.;

Supervision: K.Y.;

Project Administration: His.M., Hir.M., T.T., S.H., H.H., M.T., and M.K.;

Funding Acquisition: Tat.S.

Data availability

All data generated during this study are include in this published article and its supplementary information files..

Declaration of interests

K.S. is an employee of Tanaka Kikinzoku Kogyo K.K., and J.S. is an employee of MiCAN Technologies Inc. The authors declare no competing interests.

References

1. Wu, F. *et al.* A new coronavirus associated with human respiratory disease in China. Nature **579**, 265–269, doi:10.1038/s41586-020-2008-3 (2020).
2. Hoffmann, M. *et al.* SARS-CoV-2 Cell Entry Depends on ACE2 and TMPRSS2 and Is Blocked by a Clinically Proven Protease Inhibitor. *Cell* **181**, 271-280 e278, doi:10.1016/j.cell.2020.02.052 (2020).
3. Cheung, C. Y. *et al.* Cytokine responses in severe acute respiratory syndrome coronavirus-infected macrophages in vitro: possible relevance to pathogenesis. J Virol **79**, 7819–7826, doi:10.1128/JVI.79.12.7819-7826.2005 (2005).
4. Varga, Z. *et al.* Endothelial cell infection and endotheliitis in COVID-19. The Lancet **395**, 1417–1418, doi:10.1016/s0140-6736(20)30937-5 (2020).
5. Wang, D. *et al.* Clinical Characteristics of 138 Hospitalized Patients With 2019 Novel Coronavirus–Infected Pneumonia in Wuhan, China. Jama **323**, doi:10.1001/jama.2020.1585 (2020).
6. Jiang, Y. *et al.* Characterization of cytokine/chemokine profiles of severe acute respiratory syndrome. Am J Respir Crit Care Med **171**, 850–857, doi:10.1164/rccm.200407-857OC (2005).
7. Hojyo, S. *et al.* How COVID-19 induces cytokine storm with high mortality. Inflamm Regen **40**, 37, doi:10.1186/s41232-020-00146-3 (2020).
8. Wilson, J. G. *et al.* Cytokine profile in plasma of severe COVID-19 does not differ from ARDS and sepsis. JCI Insight **5**, doi:10.1172/jci.insight.140289 (2020).
9. Ragab, D., Salah Eldin, H., Taeimah, M., Khattab, R. & Salem, R. The COVID-19 Cytokine Storm; What We Know So Far. Front Immunol **11**, 1446, doi:10.3389/fimmu.2020.01446 (2020).
10. Burke, H. *et al.* Inflammatory phenotyping predicts clinical outcome in COVID-19. Respir Res **21**, 245, doi:10.1186/s12931-020-01511-z (2020).
11. Del Valle, D. M. *et al.* An inflammatory cytokine signature predicts COVID-19 severity and survival. Nat Med **26**, 1636–1643, doi:10.1038/s41591-020-1051-9 (2020).
12. Gabay, C. Interleukin-6 and chronic inflammation. Arthritis Res Ther **8 Suppl 2**, S3, doi:10.1186/ar1917 (2006).
13. Nikitina, E., Larionova, I., Choinzonov, E. & Kzhyshkowska, J. Monocytes and Macrophages as Viral Targets and Reservoirs. Int J Mol Sci **19**, doi:10.3390/ijms19092821 (2018).
14. Abassi, Z., Knaney, Y., Karram, T. & Heyman, S. N. The Lung Macrophage in SARS-CoV-2 Infection: A Friend or a Foe? Front Immunol **11**, 1312, doi:10.3389/fimmu.2020.01312 (2020).
15. Zhou, J., Chu, H., Chan, J. F. & Yuen, K. Y. Middle East respiratory syndrome coronavirus infection: virus-host cell interactions and implications on pathogenesis. Virol J **12**, 218, doi:10.1186/s12985-015-0446-6 (2015).

16. Yilla, M. *et al.* SARS-coronavirus replication in human peripheral monocytes/macrophages. Virus Res **107**, 93–101, doi:10.1016/j.virusres.2004.09.004 (2005).
17. Hui, K. P. Y. *et al.* Tropism, replication competence, and innate immune responses of the coronavirus SARS-CoV-2 in human respiratory tract and conjunctiva: an analysis in ex-vivo and in-vitro cultures. The Lancet Respiratory Medicine **8**, 687–695, doi:10.1016/s2213-2600(20)30193-4 (2020).
18. Port, J. R. *et al.* SARS-CoV-2 disease severity and transmission efficiency is increased for airborne compared to fomite exposure in Syrian hamsters. Nat Commun **12**, 4985, doi:10.1038/s41467-021-25156-8 (2021).
19. Tseng, C. T., Perrone, L. A., Zhu, H., Makino, S. & Peters, C. J. Severe acute respiratory syndrome and the innate immune responses: modulation of effector cell function without productive infection. J Immunol **174**, 7977–7985, doi:10.4049/jimmunol.174.12.7977 (2005).
20. Grant, R. A. *et al.* Circuits between infected macrophages and T cells in SARS-CoV-2 pneumonia. Nature **590**, 635–641, doi:10.1038/s41586-020-03148-w (2021).
21. Zhou, Y. *et al.* Pathogenic T-cells and inflammatory monocytes incite inflammatory storms in severe COVID-19 patients. National Science Review **7**, 998–1002, doi:10.1093/nsr/nwaa041 (2020).
22. Garcia-Nicolas, O. *et al.* No Evidence for Human Monocyte-Derived Macrophage Infection and Antibody-Mediated Enhancement of SARS-CoV-2 Infection. Front Cell Infect Microbiol **11**, 644574, doi:10.3389/fcimb.2021.644574 (2021).
23. Shimizu, J. *et al.* The potential of COVID-19 patients' sera to cause antibody-dependent enhancement of infection and IL-6 production. Scientific Reports **11**, doi:10.1038/s41598-021-03273-0 (2021).
24. Young, B. E. *et al.* Viral dynamics and immune correlates of COVID-19 disease severity. Clin Infect Dis, doi:10.1093/cid/ciaa1280 (2020).
25. Kang, S. *et al.* IL-6 trans-signaling induces plasminogen activator inhibitor-1 from vascular endothelial cells in cytokine release syndrome. Proc Natl Acad Sci U S A **117**, 22351–22356, doi:10.1073/pnas.2010229117 (2020).
26. Fajnzylber, J. *et al.* SARS-CoV-2 viral load is associated with increased disease severity and mortality. Nat Commun **11**, 5493, doi:10.1038/s41467-020-19057-5 (2020).
27. Sugiyama, M. *et al.* Serum CCL17 level becomes a predictive marker to distinguish between mild/moderate and severe/critical disease in patients with COVID-19. Gene **766**, 145145, doi:10.1016/j.gene.2020.145145 (2021).
28. Huang, C. *et al.* Clinical features of patients infected with 2019 novel coronavirus in Wuhan, China. The Lancet **395**, 497–506, doi:10.1016/s0140-6736(20)30183-5 (2020).
29. Gandhi, R. T., Lynch, J. B. & Del Rio, C. Mild or Moderate Covid-19. N Engl J Med **383**, 1757–1766, doi:10.1056/NEJMcp2009249 (2020).
30. Batra, M. *et al.* Role of IgG against N-protein of SARS-CoV2 in COVID19 clinical outcomes. Sci Rep **11**, 3455, doi:10.1038/s41598-021-83108-0 (2021).

31. Sun, B. *et al.* Kinetics of SARS-CoV-2 specific IgM and IgG responses in COVID-19 patients. Emerg Microbes Infect **9**, 940–948, doi:10.1080/22221751.2020.1762515 (2020).
32. Karwaciak, I., Salkowska, A., Karas, K., Dastych, J. & Ratajewski, M. Nucleocapsid and Spike Proteins of the Coronavirus SARS-CoV-2 Induce IL6 in Monocytes and Macrophages-Potential Implications for Cytokine Storm Syndrome. Vaccines (Basel) **9**, doi:10.3390/vaccines9010054 (2021).
33. Zhang, X. *et al.* Nucleocapsid protein of SARS-CoV activates interleukin-6 expression through cellular transcription factor NF-kappaB. Virology **365**, 324–335, doi:10.1016/j.virol.2007.04.009 (2007).
34. Pan, P. *et al.* SARS-CoV-2 N protein promotes NLRP3 inflammasome activation to induce hyperinflammation. Nat Commun **12**, 4664, doi:10.1038/s41467-021-25015-6 (2021).
35. Hohdatsu, T. *et al.* Antibody-dependent enhancement of feline infectious peritonitis virus infection in feline alveolar macrophages and human monocyte cell line U937 by serum of cats experimentally or naturally infected with feline coronavirus. J Vet Med Sci **60**, 49–55, doi:10.1292/jvms.60.49 (1998).
36. Ricke, D. O. Two Different Antibody-Dependent Enhancement (ADE) Risks for SARS-CoV-2 Antibodies. Front Immunol **12**, 640093, doi:10.3389/fimmu.2021.640093 (2021).
37. Tseng, C. T. *et al.* Immunization with SARS coronavirus vaccines leads to pulmonary immunopathology on challenge with the SARS virus. PLoS One **7**, e35421, doi:10.1371/journal.pone.0035421 (2012).
38. Bolles, M. *et al.* A double-inactivated severe acute respiratory syndrome coronavirus vaccine provides incomplete protection in mice and induces increased eosinophilic proinflammatory pulmonary response upon challenge. J Virol **85**, 12201–12215, doi:10.1128/JVI.06048-11 (2011).
39. Yasui, F. *et al.* Prior immunization with severe acute respiratory syndrome (SARS)-associated coronavirus (SARS-CoV) nucleocapsid protein causes severe pneumonia in mice infected with SARS-CoV. J Immunol **181**, 6337–6348, doi:10.4049/jimmunol.181.9.6337 (2008).
40. Al Kaabi, N. *et al.* Effect of 2 Inactivated SARS-CoV-2 Vaccines on Symptomatic COVID-19 Infection in Adults: A Randomized Clinical Trial. JAMA **326**, 35–45, doi:10.1001/jama.2021.8565 (2021).
41. Zhang, Y. *et al.* Safety, tolerability, and immunogenicity of an inactivated SARS-CoV-2 vaccine in healthy adults aged 18–59 years: a randomised, double-blind, placebo-controlled, phase 1/2 clinical trial. The Lancet Infectious Diseases **21**, 181–192, doi:10.1016/s1473-3099(20)30843-4 (2021).
42. Li, L. *et al.* Effect of Convalescent Plasma Therapy on Time to Clinical Improvement in Patients With Severe and Life-threatening COVID-19: A Randomized Clinical Trial. JAMA **324**, 460–470, doi:10.1001/jama.2020.10044 (2020).
43. Agarwal, A. *et al.* Convalescent plasma in the management of moderate covid-19 in adults in India: open label phase II multicentre randomised controlled trial (PLACID Trial). BMJ **371**, m3939, doi:10.1136/bmj.m3939 (2020).
44. Bégin, P. *et al.* Convalescent plasma for hospitalized patients with COVID-19: an open-label, randomized controlled trial. Nature Medicine, doi:10.1038/s41591-021-01488-2 (2021).
45. Krammer, F. *et al.* Antibody Responses in Seropositive Persons after a Single Dose of SARS-CoV-2 mRNA Vaccine. N Engl J Med **384**, 1372–1374, doi:10.1056/NEJMc2101667 (2021).

46. Anderson, E. M. *et al.* Seasonal human coronavirus antibodies are boosted upon SARS-CoV-2 infection but not associated with protection. Cell, doi:10.1016/j.cell.2021.02.010 (2021).
47. Gorse, G. J., Donovan, M. M. & Patel, G. B. Antibodies to coronaviruses are higher in older compared with younger adults and binding antibodies are more sensitive than neutralizing antibodies in identifying coronavirus-associated illnesses. J Med Virol **92**, 512–517, doi:10.1002/jmv.25715 (2020).
48. Li, K. *et al.* Dynamic changes in anti-SARS-CoV-2 antibodies during SARS-CoV-2 infection and recovery from COVID-19. Nat Commun **11**, 6044, doi:10.1038/s41467-020-19943-y (2020).
49. Lee, N. *et al.* Anti-SARS-CoV IgG response in relation to disease severity of severe acute respiratory syndrome. J Clin Virol **35**, 179–184, doi:10.1016/j.jcv.2005.07.005 (2006).
50. Liu, X. *et al.* Patterns of IgG and IgM antibody response in COVID-19 patients. Emerg Microbes Infect **9**, 1269–1274, doi:10.1080/22221751.2020.1773324 (2020).
51. Chen, W. *et al.* SARS-CoV-2 neutralizing antibody levels are correlated with severity of COVID-19 pneumonia. Biomed Pharmacother **130**, 110629, doi:10.1016/j.biopha.2020.110629 (2020).
52. Luo, Y. R., Chakraborty, I., Yun, C., Wu, A. H. B. & Lynch, K. L. Kinetics of SARS-CoV-2 Antibody Avidity Maturation and Association with Disease Severity. Clin Infect Dis, doi:10.1093/cid/ciaa1389 (2020).
53. Legros, V. *et al.* A longitudinal study of SARS-CoV-2-infected patients reveals a high correlation between neutralizing antibodies and COVID-19 severity. Cell Mol Immunol **18**, 318–327, doi:10.1038/s41423-020-00588-2 (2021).
54. Grasselli, G. *et al.* Risk Factors Associated With Mortality Among Patients With COVID-19 in Intensive Care Units in Lombardy, Italy. JAMA Intern Med **180**, 1345–1355, doi:10.1001/jamainternmed.2020.3539 (2020).
55. Masia, M. *et al.* Impact of interleukin-6 blockade with tocilizumab on SARS-CoV-2 viral kinetics and antibody responses in patients with COVID-19: A prospective cohort study. EBioMedicine **60**, 102999, doi:10.1016/j.ebiom.2020.102999 (2020).
56. Kalil, A. C. *et al.* Baricitinib plus Remdesivir for Hospitalized Adults with Covid-19. N Engl J Med **384**, 795–807, doi:10.1056/NEJMoa2031994 (2021).
57. Hiroi, S. *et al.* Infectivity assay for detection of SARS-CoV-2 in samples from patients with COVID-19. J Med Virol, doi:10.1002/jmv.27145 (2021).
58. Matsuyama, S. *et al.* Enhanced isolation of SARS-CoV-2 by TMPRSS2-expressing cells. Proc Natl Acad Sci U S A **117**, 7001–7003, doi:10.1073/pnas.2002589117 (2020).
59. Yamanaka, A., Miyazaki, K., Shimizu, J. & Senju, S. Dengue virus susceptibility in novel immortalized myeloid cells. Heliyon **6**, e05407, doi:10.1016/j.heliyon.2020.e05407 (2020).
60. Dent, S. & Neuman, B. W. Purification of coronavirus virions for Cryo-EM and proteomic analysis. Methods Mol Biol **1282**, 99–108, doi:10.1007/978-1-4939-2438-7_10 (2015).
61. Masrinoul, P. *et al.* Monoclonal antibody targeting chikungunya virus envelope 1 protein inhibits virus release. Virology **464-465**, 111–117, doi:10.1016/j.virol.2014.05.038 (2014).

Figures

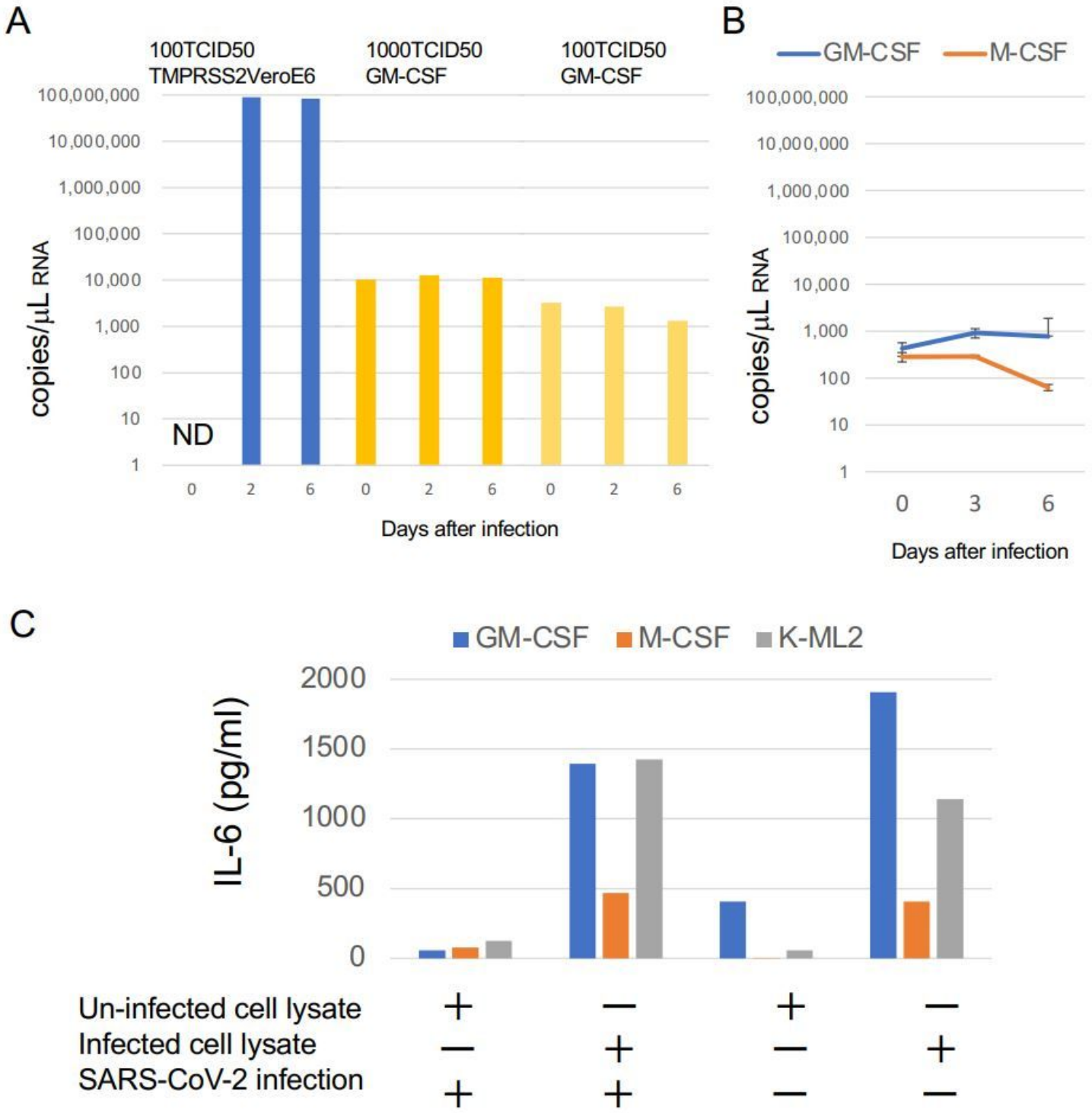

Figure 1

IL-6 production induced by SARS-CoV-2-infected cell lysate in macrophages (MDM) and iPS-derived myeloid cells without productive infection

Peripheral blood mononuclear cells were differentiated into MDM by adding GM-CSF or (B) M-CSF for 8 days. TMPRSS2/VeroE6 cells and MDM were infected with SARS-CoV-2 (A: JPN-TY-Wk-521 strain; B: KNG-19-020 strain) for 4 h, then washed once with medium. The viral RNA in the supernatants was measured by RT-PCR on the indicated days. (C) iPS-derived myeloid cells K-ML2 (gray) and MDM (blue and red were inoculated with the SARS-CoV-2 KNG-19-020 strain with SARS-CoV-2-infected or uninfected cell lysate. Four hours later, the MDM were washed once. Two days after infection, the IL-6 levels in the culture supernatants were measured by ELISA. The results of at least three representative independent experiments are shown.

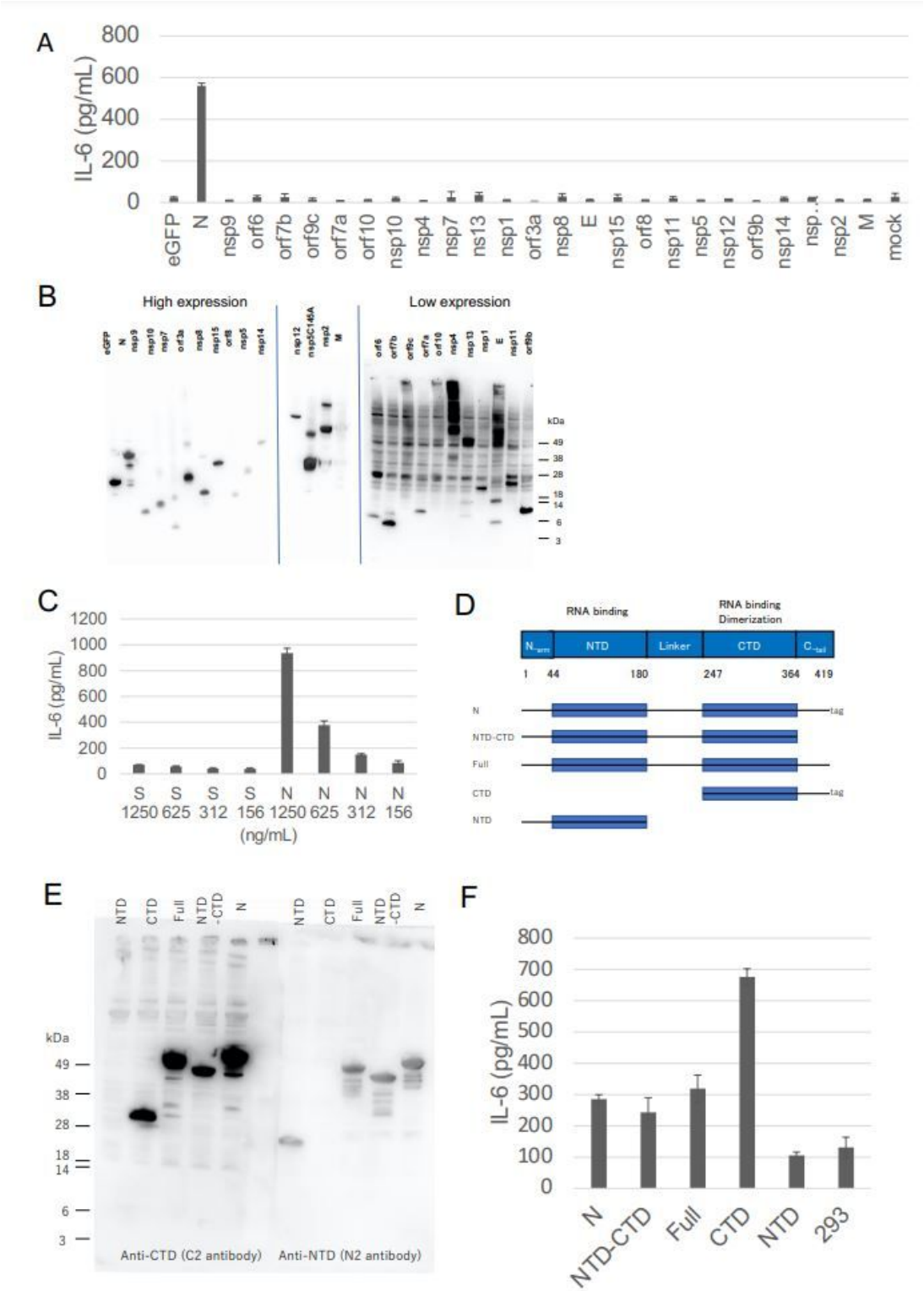

Figure 2

SARS-CoV-2 N protein, but not S protein, induced IL-6 production

The levels of IL-6 were measured by ELISA 2 days after treatment (A, C, and F). (A) K-ML2 cells were stimulated with the lysate of 293T cells transfected with plasmids encoding each of the SARS-CoV-2 proteins. (B) The expression of each viral protein was confirmed by western blot using the anti-Strep tag.

(C) K-ML2 cells were stimulated with serial diluted S or N protein produced using a baculovirus expression system. The mean and standard deviation of triplicate samples are shown. (D) A schematic diagram of full-length and truncated N proteins. (E) Anti-NTD (N2) antibody and anti-CTD (C2) antibody were used to visualize the full-length and truncated N proteins by western blot. (F) K-ML2 cells were stimulated with the cell lysates of 293T cells expressing the full-length or truncated N proteins. Data are expressed as the mean and standard deviation of triplicate samples. The results of three representative independent experiments are shown.

Figure 3

Profiles of cytokine production from macrophages (MDM) stimulated by N protein

MDM differentiated with GM-CSF or M-CSF were stimulated by 156 or 625 ng/mL of N proteins for 2 days. The cytokine levels were measured by a multiplex assay, as described in the STAR Methods. Data are expressed as the mean and standard deviation of triplicate samples.

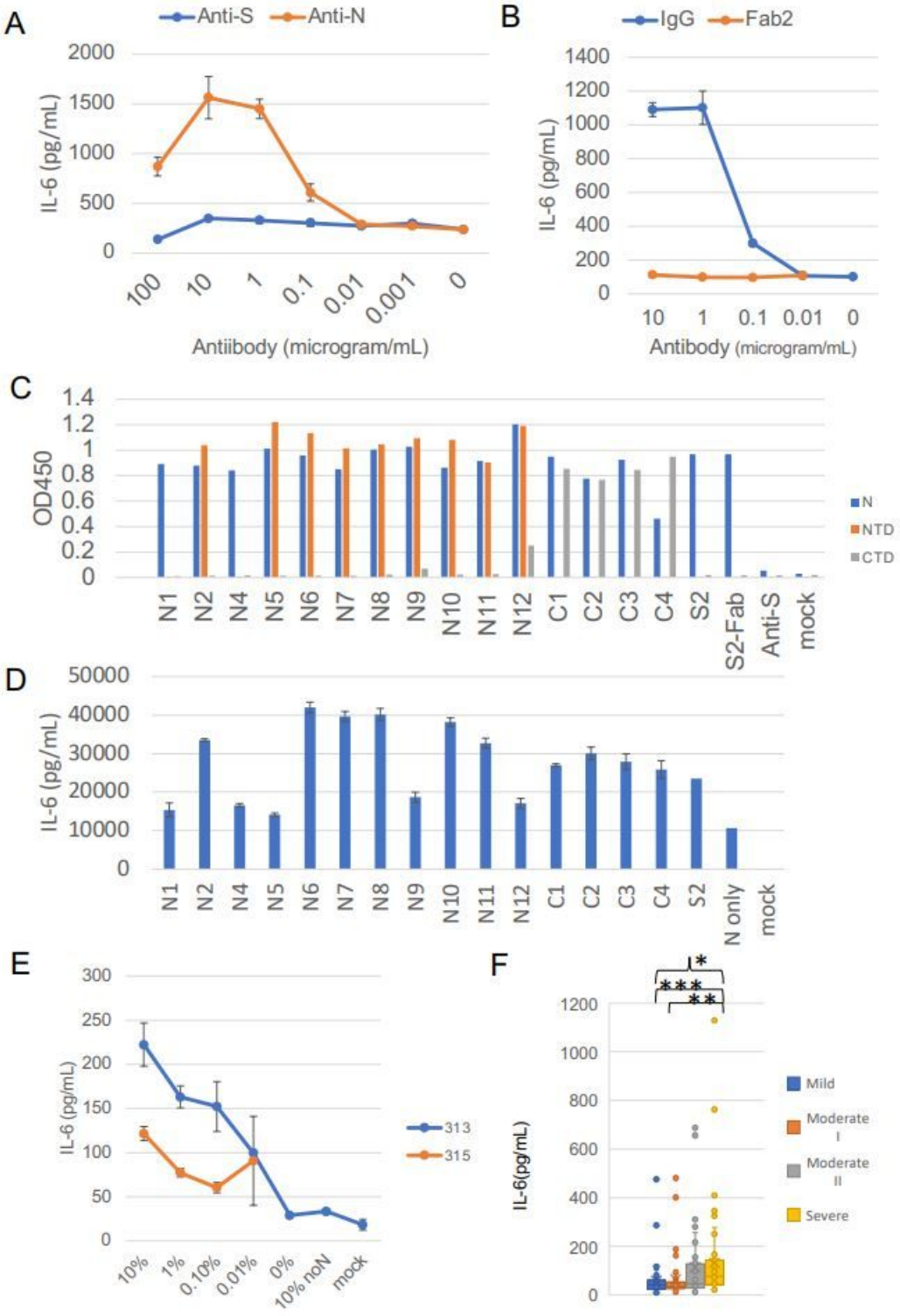

Figure 4

Anti-N antibodies and COVID-19 patient sera enhanced the IL-6 production induced by N protein

Levels of IL-6 were measured by ELISA 2 days after the addition of N protein, except for in panel C. (A) K-ML2 cells were stimulated with 156 ng/mL of N protein with escalating amounts of anti-S (blue) or anti-N (red) antibodies. (B) Anti-N antibody, S2, was digested by pepsin, and purified F(ab')2 (red) or IgG (blue)

was added to induce IL-6 production. Data are expressed as the mean and standard deviation of triplicate samples. (C) The levels of mouse mAbs bound to the full-length N protein (blue), NTD (Thr49-Gly175 fragment; red, or CTD (Lys248-Pro365 fragment; gray) were measured by an in-house ELISA. Anti-S mAb, clone 29-C7, was used as a negative control. (D) K-ML2 cells were stimulated with 3 mL of the cell lysate of N protein-expressing 293T cells in the presence of 1 mg/mL of mAbs. Data are expressed as the mean and standard deviation of triplicate samples. The results of three representative independent experiments are shown. (E) K-ML2 cells were stimulated with 156 ng/mL of N protein with escalating amounts of serum from two patients. “0%” indicates the baseline production of IL-6 induced by N protein. “10% noN” indicates the level of non-specific IL-6 induction from the addition of 10% patient serum from patient No. 313. (F) The levels of IL-6 in the culture supernatants of K-ML2 cells cultured in the presence of 1% patient serum. Specimens were divided into four groups according to the disease severity at the time of blood collection. The center lines in the boxes and the boxes indicate the median and 25/75 percentiles, respectively. “*” denotes a statistically significant difference among the four groups ($p < 0.0001$) by the Kruskal-Wallis test. “**” and “***” denote a statistically significant difference between the moderate I and severe disease groups ($p < 0.0001$) and between the mild and severe disease groups ($p < 0.0001$), respectively, by the Mann Whitney U test.

Supplementary Files

This is a list of supplementary files associated with this preprint. Click to download.

- SupplementalFigures.pdf
- TableS1.xlsx